Optimizing Disparity Candidates Space in Dense Stereo Matching

Ali M. Fotouhi [i]* and Abolghasem A. Raie[ii]

Received 22 October 2008; received in revised 12 October 2009; accepted 18 April 2011

ABSTRACT

In this paper, a new approach for optimizing disparity candidates space is proposed for the solution of dense stereo matching problem. The main objectives of this approach are the reduction of average number of disparity candidates per pixel with low computational cost and high assurance of retaining the correct answer. These can be realized due to the effective use of multiple radial windows, intensity information, and some usual and new constraints, in a reasonable manner. The new space improved by the new idea validation and correction retains those candidates, which satisfy more constraints and especially being more promising to satisfy the implied assumption in using support windows, i.e. the disparity consistency of the window pixels. To evaluate the proposed space, the weighted window is used to estimate dense disparity map in this space. The experimental results on the standard stereo images indicate an overall speedup factor of 11 and the improved disparity map.

KEYWORDS

Disparity Candidate – Radial Window – Validation and Correction – Weighted Window.

1. INTRODUCTION

Stereo vision or recognition of 3D structure from 2D images of a scene is one of the fundamental problems in machine vision. Modern applications such as 3D graphics, 3D displays and image based modeling have made it an active research area within the last few years. The main problem in stereo vision is finding corresponding pixels from two images or stereo matching. In feature-based stereo, the matching of feature elements such as edges or corners is considered and sparse disparity map is produced; while in area-based stereo, considered in this paper, the corresponding search process is first accomplished for all pixels of the images and dense disparity map is then produced.

The area-based algorithms could be also categorized into global and local ones. In global matching algorithms[1]-[7] an accumulative cost function is defined on the basis of matching constraints such as intensity consistency and disparity continuity on image line or surface. Then, by minimization of the cost function using iterative optimization[1]-[3] or dynamic programming algorithms [4]-[7], considering constraints for occlusion, ordering, uniqueness and ..., disparity in each pixel is finalized. In the local algorithms [8]-[13] pixel to pixel matching cost is computed using a determined function such as absolute of intensity difference and for decreasing ambiguity in matching process, matching cost for each disparity candidate is obtained by aggregating pixel to pixel matching costs in a supporting window area around the proposed pixel by the implied assumption of disparity consistency in the window area. In these algorithms, generally, using simple WTA (Winner Takes All) rule, disparity candidate with minimum matching cost is selected as the disparity of the proposed pixel.

Global methods lead to better results with respect to local methods; however, in these methods the algorithm of global cost function optimization is computationally expensive, and in some cases their performance is dependent on the quality of initial estimation of disparity values as well as accurate segmentation of images. Local matching algorithms have less computational complexity

i * Corresponding Author, Ali M. Fotouhi is with the Department of Electrical Engineering, Tafresh University, Tafresh, Iran (e-mail: fotouhi@aut.ac.ir).

ii Abolghasem A. Raie is with the Department of Electrical Engineering, Amirkabir University of Technology, Tehran, Iran (e-mail: raie@aut.ac.ir).

with respect to global methods; however, in these methods for the reason of the simplicity of selection process, determination of accurate matching cost is of great importance, to obtain smooth disparity map with sufficient details. Therefore, for improving results, rank cost functions [8] and adaptive window [9] [11], multiple window [11] and weighted window [12] [13] ideas have been proposed in the literature. In these methods, through massive and in some cases iterative computations for determination of size and shape of the window or weight of the pixels inside the window the matching cost is computed. In other words, all techniques mentioned above with different ideas are trying to fulfill the implied assumption in using the window, i.e. the disparity consistency of the window pixels, abbreviated as DCWP, in different regions of the image. However, in local matching algorithms finding an ideal matching cost with high discriminating power reflecting all necessary constraints of matching process and selecting the true match among a large number of candidates with arbitrary statistical information, regardless of its computational complexity, seem unreachable.

In this paper, a new approach for optimizing disparity candidates space in solving dense stereo matching problem is proposed and a new space named reduced disparity candidates abbreviated as RDC is obtained. It seems that in the new space by selecting candidates which satisfy more constraints, especially being more promising to satisfy DCWP constraint, and therefore the true disparity more probably can improve accuracy and computational performance as well. Using high assurance matched pixels [4] [7] and generalized directive pixels [5] to conduct matching process in global algorithms as well as increase accuracy and decrease computational cost supports the proposed idea. In the new space, the behavior of stereo matching in different regions of image can be observed and classified. In this paper, a new approach to improve the proposed space is presented and weighted window is used for dense disparity map estimation in this space. In section 45 of the paper, the proposed algorithm to organize RDC space is introduced. In section 3, the behavior of RDC space in different regions of image is considered. In section 4, an approach named validation and correction is proposed for improving the RDC space. Total validation of the proposed space and the results of dense disparity map estimation, using weighted window in this space, are presented in section 5. The concluding remarks are given in section 6.

2. REDUCED SPACE OF DISPARITY CANDIDATES

In dense stereo matching, the initial set of disparity candidates for each pixel is determined by usual epipolar, minimum and maximum disparity constraints. In binocular stereo with two rectified images, according to the epipolar constraint, if $d_{\min}$ is the minimum disparity and $d_{\max}$ is the maximum disparity of the matched pixels, the matching candidates of pixel p from the line l of the left image in location i, will be the pixels from the line l of the right image in locations $i-d_{\max}$ to $i-d_{\min}$. Therefore, if the left border of the image is not considered, disparity candidates set of pixel p in pixel scale is $cand_{p,\text{int}}=\{d_{\min},...,d_{\max}\}$ and the number of disparity candidates for each pixel and also the average number of disparity candidates per pixel, abbreviated as $ANCP$ and used for performance evaluation in this paper, are equal to:

$$ANCP = d_{\max} - d_{\min} + 1 \quad (1)$$

In this paper, organizing RDC space, using search space reduction algorithm, with the three main objectives is proposed: 1) to reduce the number of candidates per pixel as much as possible by eliminating noisy and unreliable candidates, 2) to retain those candidates promising to fulfill necessary matching constraints and conditions, specially DCWP, and so are the correct answer more probably, and 3) to maintain a computationally low cost procedure. For evaluating RDC space for the first objective $ANCP$ criterion and for the second objective $PPWTDC$ criterion, which presents percent of pixels without true disparity candidate, are used. Performance of different algorithms for dense disparity map estimation is usually evaluated by error threshold of one pixel, hence, in this paper, for computing $PPWTDC$ this threshold is used for counting pixels without true disparity candidate. Dense disparity map estimation using local or global stereo matching algorithms in RDC space, for the reason of simpler and more reliable search space, is possible by noticeable reduction of computational cost and higher precision.

A. Search space reduction algorithm

Radial window definition: Eight radial windows with 45^o of angle differences illustrated in Figure 1 and numbering presented in this figure are proposed. For each window and in each direction, a ray of pixels with the length of n two supporting rays in its left and right sides are considered. L_α denotes a vector with the length of n, including the intensity value of the center pixel and $n-1$ pixels in its continuance in the left image for a ray in direction α. $L_{1,\alpha}$ and $L_{2,\alpha}$ denote intensity vectors with the length of n for the two neighboring sides of the main ray for a ray in the direction of α in the left image. For instance, in Figure 1 for $\alpha=135$ and $n=5$ the pixels taking part in vector L_α are demonstrated in black color, while the pixels taking part in $L_{1,\alpha}$ and $L_{2,\alpha}$ vectors are shown in grey color. In the same way, for the matching candidate pixel in the right image, vectors R_α, $R_{1,\alpha}$ and

$R_{2,\alpha}$ are defined.

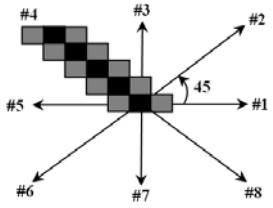

Figure 1: proposed pattern of radial windows

Matching cost function definition: The matching cost of the two pixels of p_l from the left image and p_r from the right one, in direction α, is defined as follows:

$$cost_\alpha(p_l, p_r) = \sum_{i=1}^{n}\left|\left(L_\alpha(i)+\frac{L_{1,\alpha}(i)}{2}+\frac{L_{2,\alpha}(i)}{2}\right)-\left(R_\alpha(i)+\frac{R_{1,\alpha}(i)}{2}+\frac{R_{2,\alpha}(i)}{2}\right)\right| + \sum_{i=1}^{n}\left|\left(L_{1,\alpha}(i)-L_{2,\alpha}(i)\right)-\left(R_{1,\alpha}(i)-R_{2,\alpha}(i)\right)\right|;\quad \alpha=\{0,45,...,315\} \tag{2}$$

Matching cost matrix calculations: Having calculated the matching costs of pixels for any pair of horizontal corresponding lines of the two images, using the matching cost function (2), eight matching cost matrices each belonging to one of the directions shown in Figure 1, denoted by $COST_\alpha;\ \alpha=\{0,45,...,315\}$ will be obtained.

MinMin process: In each matrix $COST_\alpha$, each point being the minimum of both the row *i* and the column *j*, which means to be satisfying left-right consistency constraint, LRCC, represent that pixel *p* in location *i* from the left image and pixel *q* in location *j* from the right one, in two corresponding horizontal lines, are the best matching candidates for each other. Therefore a reliable candidate, named $cand_{p,\alpha}=i-j$ for pixel *p* from the left image related to a ray in direction α is determined. The pixels that are not assigned a candidate in this process should mainly belong to homogenous and occluded regions; thus, being reasonable to avoid assigning them a candidate based on the matching cost.

AddLeft process: To determine the disparity candidate, $cand_{p,\alpha}$, those pixels remained unmatched through MinMin process, while they are supposed to be on the occluded or homogenous regions, on the basis of disparity continuity constraint, are assigned the exact $cand_{p',\alpha}$ of the pixel p' on the left side. Note that the pixels remained unmatched on the left side border of the image, are the exceptions of this rule and are assigned the exact $cand_{p',\alpha}$ of the pixel p' on the right.

Aggregation process: In this process, for each pixel *p*, the outputs of MinMin and AddLeft processes on the eight related matching cost matrices, namely $cand_{p,\alpha};\ \alpha=\{0,45,...,135\}$ are collected and named $cand_p$. Although $cand_p$ is a set of eight candidates for each pixel *p* of the left image, each one corresponds to one direction, note that the disparity values of these eight candidates, are not necessarily distinct and some candidates can be the same. *ANCP* is evaluated in terms of the number of distinct candidates and so after SSR algorithm its maximum value will be 8.

Comments: Two important points about using radial windows in this paper and its difference with respect to other common methods should be emphasized:

- The notion of multiple windows is used here differently from the way it is used in usual multiple-window approaches. In common multiple window methods [7][11] comparing matching cost of different windows which mask different regions of image with different statistical features is not justifiable. In the multiple window method of this paper, such comparing is not used and matching cost matrices of different windows are processed separately.
- Because of using eight slim radial windows in different directions, the probability of a continuum in which the overlapping with depth change does not occur and so DCWP constraint is satisfied, will be highly increased.

The first part of the cost function is the sum of absolute differences of intensity value of the radial window pixels of the left and right images, with the ratios indicated for main and neighboring rays. Thus, in the computation of matching cost, the intensity information of a larger area take part, which in turn cause the reduction of noise effect, especially in homogenous or repetitive textured regions. Second part of the cost function is the sum of absolute gradient differences of the intensity value of pixels of the neighboring rays in the left and right images. The less the intensity gradient difference of the radial windows of the left and right images, the less the matching cost will be. If there is a great gradient difference, and especially if the gradient direction in the specified regions of the two images is different, the matching cost will be increased. The matching cost function (2), while having low computational complexity, uses the intensity information in an effective manner.

B. RDC space representation

To represent RDC space, a one-byte number *N* between 0 and 255 is assigned to each point (*p*,*d*) of this space, which corresponds to pixel *p* of reference image with disparity candidate *d*. Based on number and position of 1s in bit string of *N*, number of repetition of disparity *d* in $cand_p$ and rays, which lead to disparity *d* by SSR algorithm, are determined. For instance, if *N* =240 is

assumed for point (*p*,*d*), its corresponding bit string, 11110000, shows that for pixel *p* four rays numbered 5, 6, 7 and 8 lead to disparity candidate *d*. On the other hand, disparity candidate *d* for pixel *p* is repeated 4 times.

In Figure 2-a, left image of stereo image "Venus" is depicted. To organize RDC space for this image, SSR algorithm with eight radial windows with length n=15 has been implemented. RDC space in determined regions in Figure 2-a for a part of a horizontal row of image has been shown with diagrams of Figure 2-b to Figure 2-f. In each diagram, columns represent the position of pixel *p* in proposed row of image and rows represent possible disparity values for proposed image based on minimum-maximum disparity constraint. To simplify representation, in intersection of column *i* and row *d* of each diagram, only repetition number of 1s in number *N* or repetition number of disparity *d* in $cand_p$ is shown and if a cell is empty, it represents that pixel *p* of the proposed row in position *i* in RDC space does not have disparity candidate *d*. It is obvious that without applying SSR algorithm all the cells in diagrams of Figure 2 have the value 1. Continuous line in diagrams of Figure 2 is obtained from true disparity map and shows true disparity values in proposed pixels of the image.

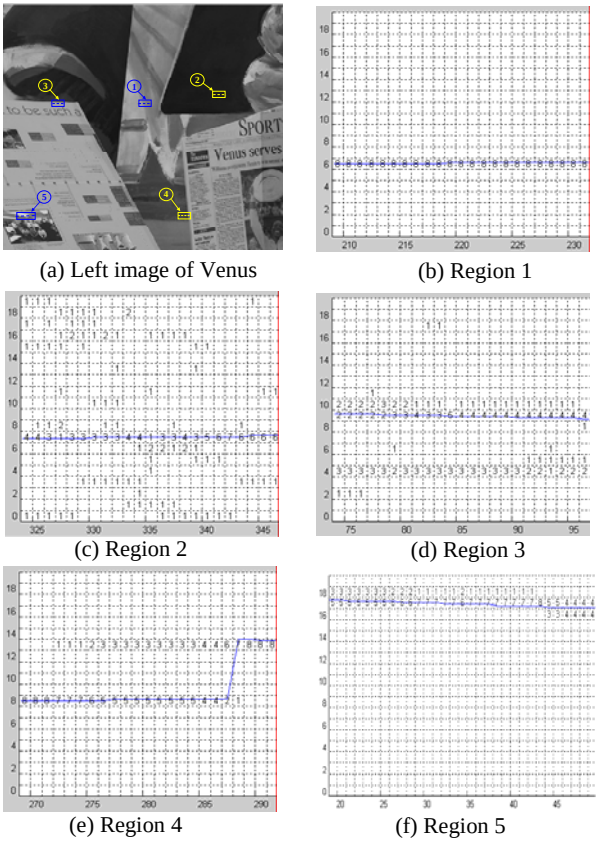

(a) Left image of Venus (b) Region 1 (c) Region 2 (d) Region 3 (e) Region 4 (f) Region 5

Figure 2: Venus image and RDC space in different regions

3. RDC SPACE DESCRIPTION IN DIFFERENT REGIONS OF IMAGE

In RDC space, most problems and complexities of stereo matching in different regions of image can be described from a different view considered in this section.

Regions with sufficient texture and without depth discontinuity: Region 1 in Figure 2-a is a sample of this type that RDC space for a part of a row of this region is presented in Figure 2-b. As observed in this region because of satisfying DCWP constraint and also existence of sufficient intensity information in radial windows, *ANCP* is equal to 1, disparity candidate in each pixel is equal to true value and *PPWTDC* is zero.

Regions with low texture and without depth discontinuity: In Figure 2-c RDC space for a part of a row of the image in region 2 is observed. Although in this region DCWP constraint is satisfied, because of low intensity information in rays, sparse disparity candidates have been produced. Representation of candidates correspond to all rays for an assumed pixel of this region in Figure 3-a shows the sparseness of disparity values for different directions. *ANCP* value in this region has been increased with respect to previous case and is equal to 5. However, for the reason of proper operation of matching cost function (2), value of *PPWTDC* is zero and in most of the pixels true value is obtained for more than three rays.

Regions near to horizontal edge with depth discontinuity: In Figure 2-d RDC space for a part of a row of image in region 3 is observed. Pixels of this region generally have two distinct disparity candidates of two far and near surfaces. On the other hand, in this region *ANCP* is approximately 2. For more precise observation of candidate distribution in this region, disparity values corresponding to all rays for an assumed pixel of this region, located on near surface, are shown in Figure 3-b. Major part of rays 2, 3 and 4 is expanded on far surface; so, for these rays DCWP constraint is violated and by SSR algorithm false disparity candidate of far surface is obtained. For other rays which are completely expanded on near surface, DCWP constraint is satisfied and obtained disparity candidates have true values.

Regions near to vertical edge with depth discontinuity: Figure 2-e shows RDC space for a part of an image row in region 4 with a vertical edge with a depth discontinuity in its continuance. In this case, as shown in Figure 3-b, for a typical pixel of this region on far surface, in rays 1, 2 and 8 which are expanded on near surface, DCWP constraint is not satisfied and so these rays lead to false disparity candidate equal to disparity of near surface. However, rays 3, 4, 5, 6 and 7 which are completely on far surface, lead to true disparity

of this surface. In such a region in left image, within depth change occurring from far surface to near surface, in some pixels of left side of depth discontinuity, a part or all of some rays occur in occlusion region. In such a case, either false disparity of near surface is assigned to these rays or by MinMin process in SSR algorithm no disparity candidate is obtained for these rays which in turn in AddLeft process are assigned usual true disparity candidate of left side pixel for the same ray. Also, in some cases, in these regions, MinMin process leads to false sparse disparity candidates. In region 4, in left side pixels of depth discontinuity for right side rays, also in right side pixels of depth discontinuity for left side rays, where a major part of the rays is expanded on far surface, disparity of this surface is expected. However, from Figure 2-e it is concluded that for these rays which overlap the near surface even for one pixel, disparity of this surface is obtained. This phenomenon is for the reason that the right side pixels of depth discontinuity on near surface have bigger intensity values and so in the cost function (2) have dominant and efficient role. This phenomenon in RDC space is equivalent to the effect of disparity propagation of near surface on far surface i.e. foreground fattening in common window methods [8]-[13].

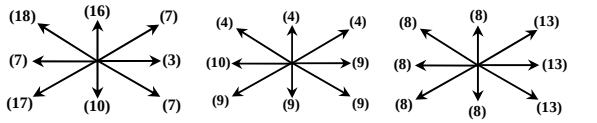

(a) Pixel 330 of Reg.2 (b) Pixel 85 of Reg.3 (c) Pixel 280 of Reg.4

Figure 3: Disparity of different rays

Slanted regions: In Figure 2-f RDC space for a part of an image row in slanted region 5 has been presented. In slanted regions, DCWP constraint is violated alongside the slant gradually and continuously; so, typically in pixels of these regions in RDC space two or more disparity candidates with adjacent values are obtained. This subject reveals the complexity of matching and the necessity of using sub-pixel estimation in these regions to extract precise disparity value [14].

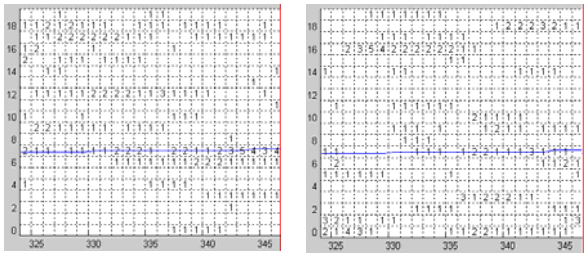

(a) Reg. 2 with simpler cost function (b) Reg. 2 with n=3

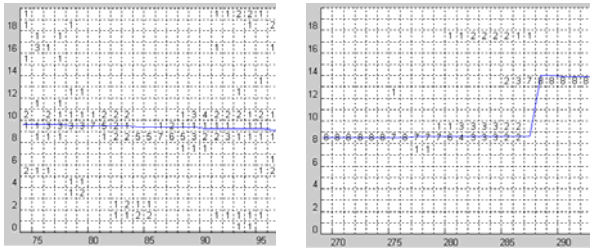

(c) Reg. 3 with n=3 (d) Reg. 4 with n=3

Figure 4: Effect of different parameters in RDC space

Important parameters to organize RDC **space:** Important parameters are matching cost function and radial window size. For instance, if the support of lateral rays for radial windows is ignored, discrimination power of matching cost function (2) is noticeably decreased. In this case, in RDC space for region 2 as shown in Figure 4-a, *ANCP* value has been increased to 6.5. To observe the effect of window size in RDC space, this space for some regions determined in Figure 2-a is represented in Figure 4 with n=3. Figure 4-b reveals that, in smooth and un-textured region 2 by decreasing the size of window, *ANCP* value is increased from 5 to 5.9 and *PPWTDC* value is increased from 0 to %30. In Figure 4-c for region 3 adjacent to a horizontal depth change, because of decreasing length of rays, DCWP constraint is satisfied for rays and therefore disparity candidates aggregate near the true value. In Figure 4-d for region 4 with a vertical depth discontinuity, decreasing length of rays causes DCWP constraint to be reserved to nearer distances of depth change edges and so the range, in which disparity candidates have two distinct values of far and near surfaces, has been decreased. Instead, increasing occlusion effect in this region causes sparse candidates near depth discontinuities. Equivalently in common window methods, with decreasing window size, disparity values will be improved to nearer distances of borders or foreground fattening is decreased; however, in smooth regions more false matches is obtained.

4. RDC SPACE IMPROVEMENT BY VALIDATION CORRECTION ALGORITHM

In this section, the new proposed algorithm named validation-correction, or "ValCor" is proposed for more processing candidates obtained for each pixel in RDC space and organizing IRDC space. The aim of ValCor process is to reduce *ANCP* , by eliminating non-valid noisy candidates, and also to decrease *PPWTDC* , by inserting new valid non-present ones and briefly to improve RDC space.

The ValCor process is done on the basis of DCWP constraint, meaning that the cost aggregation in the support window area for a pixel may be valid if most of the pixels within the window have the same disparity as

the disparity of the proposed pixel. Thus, the validity of a disparity candidate related to a ray is considered as the percent of pixels within the ray having a candidate with the same disparity value. In case a disparity candidate is supported by several rays, its validity is considered as the maximum validity computed for all rays. If the calculated validity for a candidate is less than a threshold value, this candidate will be eliminated from the list of candidates for the nominated pixel. This stage of the ValCor process is known as "validation".

Because the necessary computations to determine the disparity are performed in the pixel scale, while the disparity amounts especially on slanted surfaces can be on a sub-pixel scale, the validity of d_p+1 and d_p-1 for the rays having d_p candidate, is also calculated. Providing that these new disparity values have sufficient validity, they will be added to the list of disparity candidates for the nominated pixel. This part of the algorithm is known as the "correction". Considering $cand_{p,vc}=cand_p$ for each pixel p in the beginning of ValCor process, the steps of this process to organize IRDC space are as follows:

The computation of validity for each disparity candidate: The validity of disparity candidate shown by $v(d_p)$, is computed as:

$$v(d_p)=\underset{\alpha\in S}{MAX}\left\{\frac{1}{N_R}\sum_{\bar{p}\in R_\alpha}B(cand_{\bar{p}},d_p)\right\} \quad (3)$$

In (3), S is the set of directions which support disparity candidate d_p. R_α is the region from the left image occurring in the radial window located in pixel p and direction α. N_R is the total number of pixels present in this region, and $cand_{\bar{p}}$ is the set of disparity candidates for pixel $\bar{p}$ of this region. Function B is defined as:

$$B(cand_{\bar{p}},d_p)=\begin{cases}1 & \exists d_{\bar{p}}\in cand_{\bar{p}},\ d_{\bar{p}}=d_p\\ 0 & otherwise\end{cases} \quad (4)$$

The elimination of disparity candidate with low validity: The disparity candidate d_p for pixel p will be eliminated from disparity candidates list of pixel p if its validity is less than a threshold value of T. That is to say:

$$v(d_p)<T \Rightarrow d_p\notin cand_{p,vc} \quad (5)$$

Correction: The validity of disparity candidates of d_p+1 and d_p-1 for rays to which d_p is respected, can be computed from (3). If the amount of validity of each of them is greater than the threshold T, then the same amount will be added to $cand_{p,vc}$, i.e. the set of disparity candidates of pixel p. In other words:

$$v(d_p\pm1)>T \Rightarrow (d_p\pm1)\in cand_{p,vc} \quad (6)$$

ValCor process effect: The result of applying ValCor process on RDC space in Venus image, with threshold value T=0.75, for some regions of Figure 2-a is shown in Figure 5. IRDC space in Figure 5-a and comparing it with Figure 2-c reveal that in un-textured region 2 *ANCP* value is decreased from 5 to 1.7 because of eliminating sparse candidates in validation stage, while true candidates have enjoyed the support of adjacent pixels based on disparity continuity constraint and so have been reserved. In the regions adjacent to depth discontinuity, disparity candidates with the disparity value of one of surfaces neighboring depth discontinuity will be reserved and other sparse candidates will be eliminated. This subject is confirmed by observing IRDC space in Figure 5-b for region 3 adjacent to a horizontal depth discontinuity and comparing it with Figure 2-d. IRDC space for Figure 2-e has remained unchanged; however, considering IRDC space in Figure 5-c for region 4, using radial windows with length 3, and comparing it with Figure 4-d reveals that sparse candidates in occlusion region have been eliminated. In Figure 5-d IRDC space is presented for slanted region 5. Comparing it with Figure 2-f reveal that in this case correction stage of ValCor process leads to adding disparity candidates in some pixels. In simple case, if disparity value of each pixel in this region is assumed average value of all disparity values for that pixel, it will be considered that, using ValCor process, the results of disparity estimation will be closer to the real values.

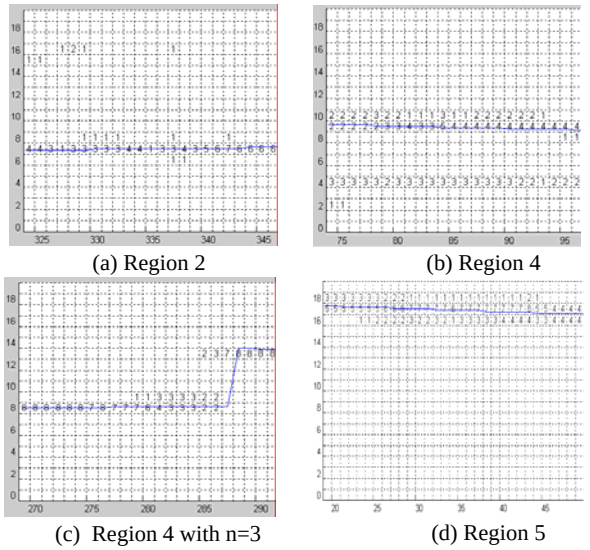

(a) Region 2 (b) Region 4

(c) Region 4 with n=3 (d) Region 5

Figure 5: RDC space after applying ValCor process

5. EXPERIMENTAL RESULTS

In section 2, three major objectives were enumerated in configuring reduced space of disparity candidates. In this section, the proposed objectives in IRDC space, also the main purpose which is the improvement of dense disparity map are evaluated for standard stereo images "Tsukuba", "Sawtooth", "Venus" and "Map", generally used to compare different algorithms [15]. In Figure 6-a, left images and in Figure 6-b, ground truth disparity maps of these stereo images are presented. IRDC space is organized with eight radial windows of length n=15 and threshold value of T=0.75 in ValCor algorithm.

A. Evaluation of Search Space Reduction Stage

In this section the first objective in IRDC space, i.e. disparity candidate reduction ratio, is evaluated. For this purpose, the average number of distinct disparity candidates for each pixel, $ANCP$, before organizing IRDC space, as computed from (1), for each image is presented in the first row of Table 1. The value of $ANCP$, in IRDC space, is presented in the second row of Table 1. The last row of the table shows the reduction ratio of $ANCP$ for each image. Significant reduction ratio from 8.2 to 16.2 with the average of 11 on the standard benchmarks represents remarkable achievement on the first objective in IRDC space. In reduction of $ANCP$, SSR and ValCor algorithms have different behavior. For instance, for "Venus" image after the SSR algorithm, the value of $ANCP$ reduces from 20 to 2.08 and using ValCor process reduces to 1.91. Although, reduction of candidates due to the latter process compared to the preceding one is not noticeable, it should be noted that after ValCor process validated candidates are selected, while the process of correction, which in turn, may cause an increase in the number of candidates, is carried out.

TABLE 1
PERFORMANCE OF SERACH SPACE REDUCTION ALGORITHM

	Tsukuba	Sawtooth	Venus	Map
Initial $ANCP$	16	20	20	30
$ANCP$ in IRDC space	1.94	1.87	1.91	1.85
Reduction Ratio	8.2	10.7	10.5	16.2

B. Dense disparity map estimation in IRDC space

To estimate dense disparity map in IRDC space, disparity of each pixel is selected using an efficient matching cost function. In this paper, weighted window, proposed in [13] leads to better results with respect to other methods, is used. In the weighted window method bigger weight is assigned to pixels of the window being more probable to have a disparity equal to that of the center pixel. The most important shortcoming of the weighted window method is its high computational cost for the reason of using large windows and calculating weights with complicated mathematical functions [6][13]. From section 5.A, it is concluded that in IRDC space, complicated computations of weighted window for standard stereo images is reduced 11 times in average. Using parameters proposed in [13] for weighted window dense disparity map estimation in initial set of candidates and also in IRDC space are presented in

Table 2. Numbers in the table are error percent with threshold value of one pixel in non-occluded, un-textured and near depth discontinuity regions. In Map image, there is no un-textured region. To correct the disparity values in the pixels of occluded regions and border of image, LRCC process is used [16]. Obtained dense disparity maps using SSR for different test images are depicted in Figure 6-c. To compare, the first and the third rows of Table 3 show the percent of error without IRDC space and in IRDC space, for all image. To see the effect of ValCor process in IRDC space, the second row of Table 3 presents the results of algorithm in RDC space.

The percent of pixels without true disparity candidate, $PPWTDC$, can determine the lower bound of final error of dense disparity map estimation in IRDC space; however, considering experimental results reveals that the share of IRDC space of total error is really negligible and is in average 10 percent, meaning quite acceptable fulfillment of the second objective in IRDC space. On the other hand, applying weighted window in IRDC space, due to choosing the validated candidates which fulfill more constraints and eliminating the noisy ones, leads to more precise results. Comparing the results of the Table 2 in different regions of image confirms this reality and also comparing the results of the first and the third rows of Table 3 reveals that in IRDC space the overall error of dense disparity map estimation error is reduced by the average percent of 25 on different images. The comparison of the first row of Table 3 with its second row shows that applying weighted window in RDC space in some cases; e.g. Tsukuba image, increase the error and so error reduction in IRDC space revels that correction phase of ValCor process has a considerable effect on the compensation of $PPWTDC$.

C. Computational cost

All calculations in the processes of SSR and ValCor algorithms to organize IRDC space are based on simple mathematical operations including add, subtract, compare and shift operations on integer numbers with the capability of parallelism. For instance, considering the number of required operations and functions and their execution times in Visual C++6, on the Intel P4 2.66GHz PC, and without parallelism, the ratio of computational cost per pixel to organize IRDC space, ($CPirdc$) and weighted window ($CPww$) is found to be $CPirdc$ / $CPww$ =25/10000. if $CCww$

and *CPirdc -ww* represent respectively the total computational cost of dense disparity map estimation in initial set of disparity candidates and IRDC space the following equations hold:

$$CC_{ww} = N_p * CP_{ww} * D_r \quad (7)$$

$$CC_{irdc-ww} = N_p * CP_{rdc} * D_r + N_p * CP_{ww} * D_r / R_c \quad (8)$$

$$CC_{irdc-ww} / CC_{ww} = 25/10000 + 1/R_c \approx 1/R_c \quad (9)$$

6. CONCLUSION

In this paper by effective use of usual information and constraints in stereo vision, new space of RDC space to solve dense stereo matching problem was proposed. To organize new space, intensity information in multiple radial windows, left-right consistency constraint, disparity continuity constraint and new DCWP constraint were employed. The main properties of this space were; significant reduction of search space and retaining the correct answer amongst remaining candidates, without complicated computational calculations. By organizing this reduced space observing stereo matching complications is provided from a different and simpler view. By proposing RDC space in this paper, three research paths in solving dense stereo matching problems are opened: 1) suggestion of ideas to improve the new space considering its basic objectives. 2) Applying previous dense stereo matching algorithms in new space and considering their performance from the view points of accuracy and run time in this space. 3) Suggesting new algorithms in proposed space to estimate dense stereo map. In this paper, in the first path an algorithm to improve RDC space and to organize IRDC space was presented and in the second path weighted window method was used for final decision making about disparity of each pixel in IRDC space. Experimental results indicate an overall speedup factor of 11 and % 25 error reductions in dense disparity map estimation with respect to the case without using the proposed space.

TABLE 2
PERFORMANCE OF DENSE STERO MATCHING BASED ON WEIGHTED WINDOW AND WTA IN IRDC SPACE

	Tsukuba			Sawtooth			Venus			Map	
	nonocc	untex	disc	nonocc	untex	disc	nonocc	untex	disc	nonocc	disc
In initial space	3.21	2.95	7.92	1.32	0.29	5.32	2.63	3.39	7.65	1.62	11.46
In IRDC space	2.49	2.76	8.57	1.12	0.23	5.04	1.04	0.94	6.88	0.66	7.70

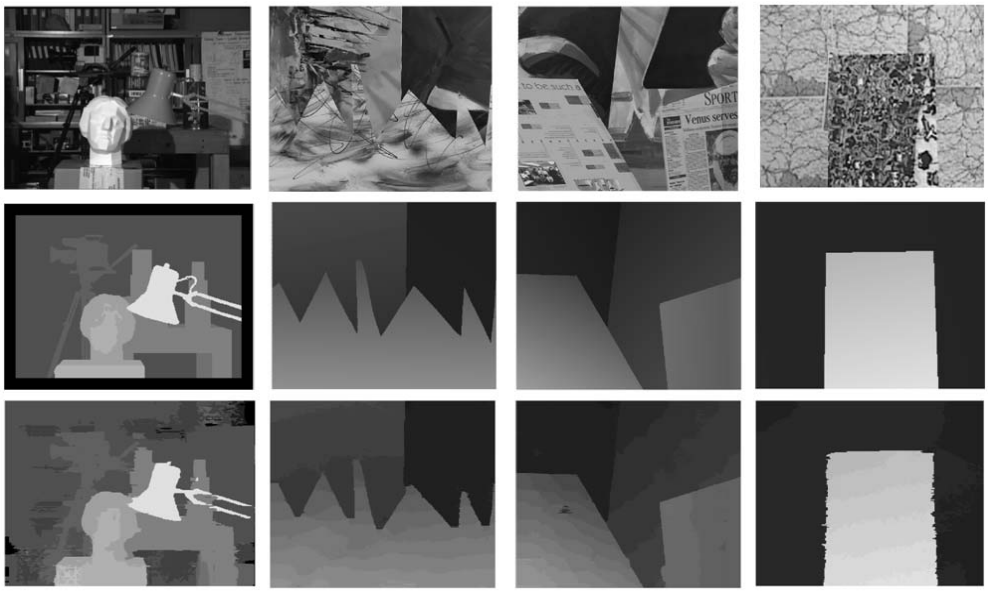

(a) (b) (c)

Figure 6: (a) Left image, (b) True disparity map, (c) Results in IRDC space

TABLE 3
WEIGHTED WINDOW AND LRCC PERFORMANCE IN DIFFERENT STATES

	Tsukuba	Sawtooth	Venus	Map
In initial space	3.25	1.80	1.61	1.67
In RDC space	3.60	1.62	1.01	1.12
In IRDC space	2.92	1.60	0.80	1.06

7. REFERENCES

[1] Lin MH, Tomasi C, "Surfaces with occlusions from layered stereo", IEEE Transactions on Pattern Analysis and Machine Intelligence, Vol 26(8), 2004.

[2] Q. Yáng, L. Wang, R. Yang, H. Stewénius, and D. Nistér. "Stereo matching with color-weighted correlation, hierarchical belief propagation and occlusion handling", IEEE Transactions on Pattern Analysis and Machine Intelligence, Vol. 31(3): 492-504, 2009.

[3] Y. Taguchi, B. Wilburn, and L. Zitnick, "Stereo reconstruction with mixed pixels using adaptive over-segmentation", In Proc. of the IEEE International Conference on Computer Vision and Pattern Recognition (CVPR), pages: 1-8, 2008.

[4] P.H.S. Torr, A. Criminisi, "Dense stereo using pivoted dynamic programming", **ELSEVIER, IMAGE AND VISION COMPUTING, VOL. 22: 795–806, 2004.**

[5] **KIM J. BOBICK, KYOUNG T., BYOUNG T. AND SANG L. "A DENSE STEREO MATCHING USING TWO-PASS DYNAMIC PROGRAMMING WITH GENERALIZED GROUND CONTROL POINTS", IEEE CONF. COMPUTER VISION AND PATTERN RECOGNITION (CVPR). 19/05: 1063-69, 2005.**

[6] **WANG, LIANG; LIAO, MIAO; GONG, "HIGH-QUALITY REAL-TIME STEREO USING ADAPTIVE COST AGGREGATION AND DYNAMIC PROGRAMMING". THIRD INTERNATIONAL SYMPOSIUM ON 3D DATA PROCESSING, VISUALIZATION, AND TRANSMISSION, PAGE(S):798 – 805, 2006.**

[7] Aaron F. Bobick and Stephen S. Intille. "Large occlusion stereo", International Journal of Computer Vision, Vol . 33(3): 181-200, 1999.

[8] Dinkar N.Bhat Shree K. Nayar , "Ordinal Measures for visual Correspondence", IEEE Transactions on Pattern Analysis and Machine Intelligence, Vol. 20(4): 415-423, 1998.

[9] Takeo Kanade and M. Okutomi. "A stereo matching algorithm with an adaptive window: Theory and experiment", IEEE Transactions on Pattern Analysis and Machine Intelligence, Vol .16(9):920-932, 1994.

[10] Olga Veksler "stereo correspondence With Compact Windows via Minimum Ratio Cycle", IEEE Transactions on Pattern Analysis and Machine Intelligence, Vol . 24(12): 1654-1660, 2002.

[11] Heiko Hirschmuller, Peter R. Innocent, and Jon Garibaldi. "Real-time correlation based stereo vision with reduced border errors", International Journal of Computer Vision, Vol . 47: 229-246, 2002.

[12] T. Darrel, "A Radial Cumulative Similarity Transform for Robust Image Correspondence", Proc. IEEE Conf. Computer Vision and Pattern Recognition(CVPR), 656-662, 1998.

[13] K.-J. Yoon and I.-S. Kweon. "Adaptive support-weight Approach for Correspondence Search", IEEE Trans.on Pattern Analysis and Machine Intelligence, Vol. 28(4): 650-656, 2006.

[14] Abhijit Ogale ,Yiannis Aloimonos. "Stereo correspondence with slanted surfaces: critical implications of horizontal slant". IEEE Conf. Comp. Vision and Pattern Recognition: 568-573, 2004.

[15] Daniel Scharstein and Richard Szeliski. "A taxonomy and evaluation of dense two-frame stereo correspondence algorithms", International Journal of Computer Vision, Vol. 47: 7-42, 2002.

[16] Geoffrey Egnal and Richard P.Wildes, "Detecting Binocular Half-Occlusions: Empirical Comparisons of Five Approaches", IEEE Trans.on Pattern Analysis and Machine Intelligence, Vol. 24(8): 1127-1133, 2002.